Available online at www.sciencedirect.com
SCIENCE DIRECT
International Journal of Heat and Mass Transfer 49 (2006) 3477–3486
International Journal of HEAT and MASS TRANSFER
www.elsevier.com/locate/ijhmt

Effects of jet plate size and plate spacing on the stagnation Nusselt number for a confined circular air jet impinging on a flat surface

Jung-Yang San *, Wen-Zheng Shiao

Department of Mechanical Engineering, National Chung-Hsing University, 250 Kuo-Kuang Road, Taichung, Taiwan, Republic of China

Received 23 September 2005; received in revised form 28 February 2006
Available online 23 May 2006

Abstract

This work deals with the effects of jet plate size and plate spacing (jet height) on the heat transfer characteristics for a confined circular air jet vertically impinging on a flat plate. The jet after impingement was restricted to flow in two opposite directions. A constant surface heat flux of 1000 W/m^2 was arranged. Totally 88 experiments were performed. Jet orifices individually with diameter of 1.5, 3, 6 and 9 mm were adopted. Jet Reynolds number (Re) was in the range 10,000–30,000 and plate spacing-to-jet diameter ratio (H/d) was in the range 1–6. Eleven jet plate width-to-jet diameter ratios ($W/d = 4.17$–41.7) and seven jet plate length-to-jet diameter ratios ($L/d = 5.5$–166.7) were individually considered. The measured data were correlated into a simple equation. It was found that the stagnation Nusselt number is proportional to the 0.638 power of the Re and inversely proportional to the 0.3 power of the H/d. The stagnation Nusselt number was also found to be a function of $\exp[-0.044(W/d) - 0.011(L/d)]$. Through comparisons among the present obtained data and documented results, it may infer that, for a jet impingement, the impingement-plate heating condition and flow arrangement of the jet after impingement are two important factors affecting the dependence of the stagnation Nusselt number on H/d.

Keywords: Impinging jet; Heat transfer; Stagnation Nusselt number

1. Introduction

Jet impingement is an effective technique to generate a high cooling rate on the surface of a hot object. In steel or glass industry, impinging jets are used to quench products after rolling. In gas turbine engines, impinging jets are applied for cooling of turbine blades/vanes. In laser/plasma cutting processes, with jet impingement cooling, thermal deformation of products can be reduced. Besides the above applications, impinging jets are also adopted to enhance electronic cooling.

Jambunathan et al. [1] did a detailed survey on jet impingement cooling. They concluded that the simplest correlation for local heat transfer coefficient is a function of jet Reynolds number (Re), jet height-to-jet diameter ratio (H/d), radial distance-to-jet diameter ratio (r/d) and Prandtl number (Pr). Goldstein and Behbahani [2] defined a recovery factor to express the non-dimensional adiabatic wall temperature. The recovery factor was found dependent on the plate spacing-to-jet diameter ratio, but irrelevant to the jet Reynolds number. Goldstein et al. [3] investigated the effect of entrainment on the heat transfer to a circular air jet impinging on a flat plate. They found that both the Nusselt number and heat transfer effectiveness would not be affected by the temperature difference between the ambient air and jet.

Bouchez and Goldstein [4] investigated the impingement cooling of a circular jet with/without a cross flow. The result shows that, for a moderate jet-to-cross flow mass flux ratio, the jet was deflected by the cross flow. Sparrow et al. [5] also investigated the heat transfer of a confined jet impingement with a cross flow. It was found that the convective heat transfer coefficient for case with jet impingement could be tenfold that without jet impingement.

* Corresponding author. Tel.: +886 011 4 2220/5585; fax: +886 011 4 2285/1941.
E-mail address: jysan@dragon.nchu.edu.tw (J.-Y. San).

0017-9310/$ - see front matter © 2006 Elsevier Ltd. All rights reserved.
doi:10.1016/j.ijheatmasstransfer.2006.02.055

Nomenclature

d	jet diameter (m)	U	jet mean velocity (m/s)
h	convective heat transfer coefficient (W/m^2 K)	W	jet plate width or heated surface width (m)
H	jet plate-to-impingement plate spacing (m)	x	x-coordinate (m)
k	thermal conductivity of air (W/m K)	y	y-coordinate (m)
L	jet plate length (m)		
Nu	local Nusselt number, hd/k	*Greek symbols*	
Pr	Prandtl number, v/α	α	thermal diffusivity (m^2/s)
q	surface heat flux (W/m^2)	v	kinematic viscosity (m^2/s)
Re	jet Reynolds number, Ud/v		
T_{aw}	adiabatic wall temperature (°C)	*Subscript*	
T_w	local wall temperature (°C)	sg	stagnation point

Goldstein et al. [6] performed an experiment on a confined circular jet with/without a cross flow. They concluded that, at large plate spacing, the cross flow diminishes the heat transfer coefficient; at small plate spacing, the cross flow would increase the peak heat transfer coefficient.

Sparrow et al. [7] developed an analogy technique, by measuring the amount of sublimation of naphthalene on a jet impingement surface, for evaluation of the convective heat transfer coefficient. It was found that the dimensionless mass transfer coefficient varies with the 0.8 power of the jet Reynolds number. An optical technique developed by Goldstein and Timmers [8] and Goldstein and Franchett [9] was used in measuring the heat transfer of an impinging jet with different inclined angles. The isothermal lines on the impingement plate were clearly observed. Huang and EL-Genk [10] investigated the heat transfer of an unconfined jet with low jet Reynolds numbers and small jet height-to-jet diameter ratios. The average Nusselt number was found proportional to $Re^{0.76}$. San et al. [11] performed an experiment on the local Nusselt number for a confined circular air jet vertically impinging on a flat plate. It was found that the local Nusselt number is proportional to $Re^{0.638}$. Lytle and Webb [12] performed a heat transfer measurement for an impinging jet with jet height-to-jet diameter ratios less than 1.0. The result indicates that the stagnation Nusselt number is proportional to the 0.53 power of the jet Reynolds number and -0.191 power of the jet height-to-jet diameter ratio. Li and Garimella [13] investigated the stagnation and area-averaged Nusselt numbers for a confined jet impinging on a small and discrete heat-source area. The stagnation Nusselt number was found proportional to the 0.444 power of the Prandtl number and 0.483 power of the jet Reynolds number.

Garimella and Rice [14] and Fitzerald and Garimella [15] performed experiments to examine the flow field of a confined jet impingement. A toroidal recirculation-flow pattern in the downstream was clearly shown. Angibletti et al. [16] investigated the flow field and heat transfer for a jet impinging on a flat plate. The flow structure was used to interpret the heat transfer characteristics of the jet impingement. Narayanan et al. [17] investigated the flow and heat transfer characteristics of a slot jet impinging on a flat plate. The result indicates that, for transitional jet impingement, the heat transfer coefficient monotonically decays in the flow direction; for potential-core jet impingement, a secondary peak in heat transfer appears at 3.2 times the hydraulic diameter from the jet centerline. Zhou and Lee [18] performed an experiment on the heat transfer of an impinging jet with a mesh screen installed in front of jet nozzle. The result shows that, with the mesh screen, the heat transfer can be slightly upgraded.

Huber and Viskanta [19] investigated the effect of jet-to-jet spacing on the heat transfer for a confined impinging jet array. It was found that, for large plate spacing, jet interference causes a significant degradation of the heat transfer. San and Lai [20] had also investigated the effect of jet interference on the heat transfer for staggered arrays of impinging jets. An optimum jet-to-jet spacing of heat transfer was found. Dano et al. [21] investigated the effect of nozzle geometry on the heat transfer for an in-lined array of impinging jets. The heat transfer performance of the cusped ellipse nozzle appears to be superior to that of the circular nozzle.

From the results indicated in the literature, besides nozzle geometry and jet Reynolds number, the heat transfer characteristics of a confined jet are also dependent on geometry of jet plate and that of impingement plate. Yet, up to date, this geometry effect on the heat transfer has not been thoroughly investigated. This leaves a blind spot in design of jet-impingement cooling systems. In this work, the stagnation Nusselt number of a confined circular air jet vertically impinging on a flat plate (Fig. 1) was investigated. Jet Reynolds number (Re), jet plate width-to-jet diameter ratio (W/d), jet plate length-to-jet diameter ratio (L/d) and plate spacing-to-jet diameter ratio (H/d) were treated as variables. The main objective of this work was to realize the effects of plate spacing, jet plate width and length on the jet-impingement heat transfer. To this end, it expected that the measured data of stagnation Nusselt number could be correlated into a simple function using

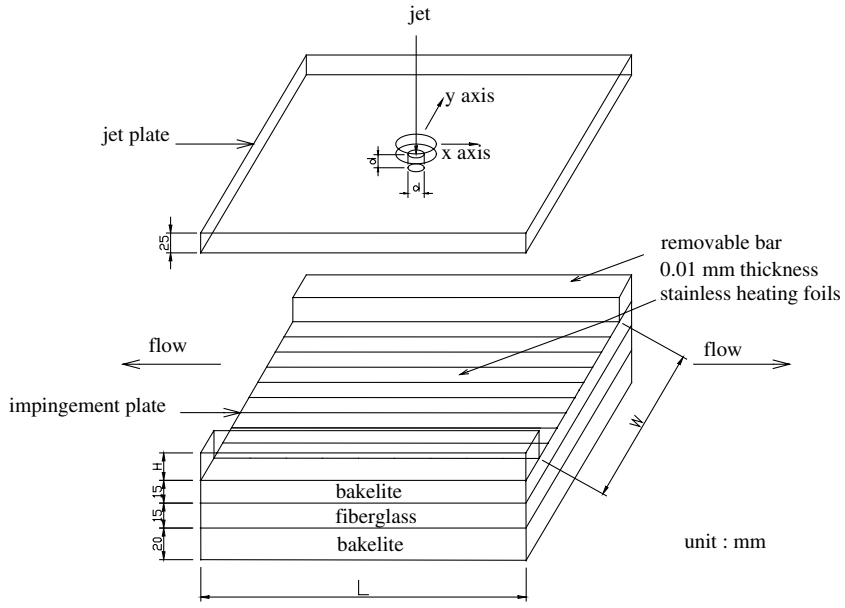

Fig. 1. Jet and impingement plates.

the above parameters. The obtained correlation will be useful to apply the impinging jet for electronic cooling.

2. Local Nusselt number

The local heat transfer coefficient, h, for a confined circular air jet impinging on a constant heat-flux plate is a function of several variables. This local heat transfer coefficient, combined with k and d, forms a local Nusselt number (Nu). As indicated in previous work [2], this local Nusselt number is relevant to heated-surface geometry, surface heat flux, jet diameter, plate spacing, location on impingement plate, jet velocity, exit flow direction and orifice aspect ratio, etc. Among these variables, the surface heat flux had been verified to be almost irrelevant to the local Nusselt number [2,11]. Thus in the analysis this variable was excluded and a fixed value equal to 1000 W/m^2 was employed. Besides that, in this work, the aspect ratio of jet orifice was selected as 1.0; the jet flow after impingement was restricted to leave through two opposite sides. With these specifications, the remaining variables can be grouped into several non-dimensional parameters. These parameters are the H/d, W/d, L/d, Re, x/d and y/d. Hence, the local Nusselt number can be expressed as follows:

$$Nu = hd/k = [q/(T_w - T_{aw})](d/k) = f(H/d, Re, W/d, L/d, x/d, y/d) \quad (1)$$

As indicated above, the function of the local Nusselt number is quite complex. For simplicity of this analysis, only the measured heat transfer data at the stagnation point ($x = y = 0$) were investigated. In this work, the considered H/d value was in the range 1–6; the Re value was in the range 10,000–30,000; the W/d value was in the range 4.17–41.7 and the L/d value was in the range 5.5–166.7.

3. Apparatus and experimental procedure

The experimental set-up for the measurement is shown in Fig. 2. During operations, a large reciprocating air compressor supplied the high-pressure air for jet impingement. This high-pressure air was stored in a large surge tank. The air pressure in this tank was in the range 7–8 atm. A pressure regulator was installed at the exit of the tank to stabilize the pressure of the supply air. In the air supply line, two vapor-compression type dehumidifiers and three adsorption columns filled with granular activated carbon were individually used for dehydration and oil removal. After the air passed through the dehumidifiers and adsorption columns, it was stored in another large surge tank. The air pressure in this tank was maintained at 4 atm. At the exit of this surge tank, there was another pressure regulator to control the exit air pressure. The volumetric flow rate of the air before delivered to the jet plate was measured using a calibrated rotameter.

The configurations of the jet plate and impingement plate are individually shown in Fig. 1. Nine 0.01 mm-thickness stainless heating foils were stuck on the impingement plate. During operations, the high-pressure air passed through the jet orifice directly impinging on the middle heating foil. The jet after impingement was restricted to flow in two opposite directions parallel to the x-axis. An electric current, supplied by an Agilent E3610A DC power supply, was arranged to flow through the heating foils to generate a uniform surface heat flux. The width of each heating foil was 12.5 mm and the length was 400 mm. Seventy-six thermocouples were orderly embedded below the middle heating foil. The spacing between any two neighboring thermocouples was 3 mm.

The jet plate was designed to be able to move in the x and y directions (Fig. 1) individually by adjusting two

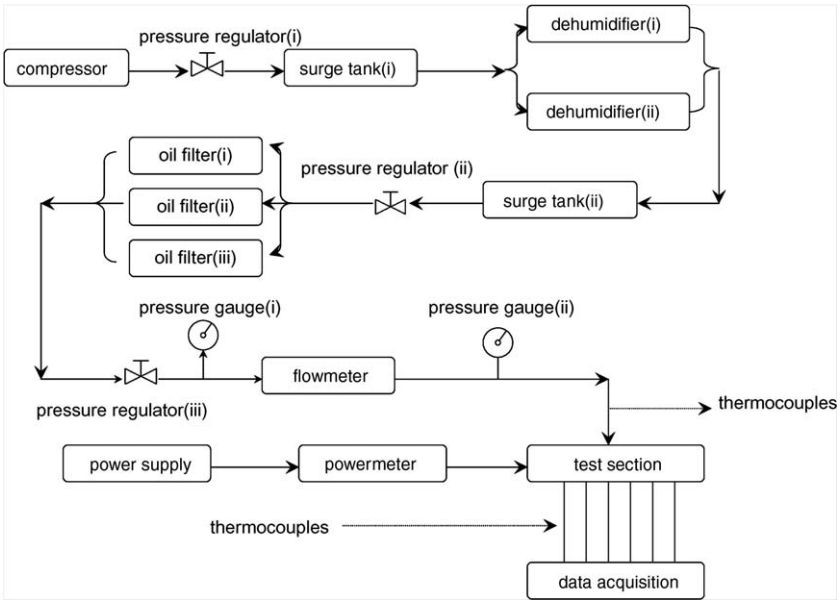

Fig. 2. Experimental set-up.

Fig. 3. Wiring of heating foils.

screws. Two linear photo-electronic scales with a smallest readout of 0.001 mm were used to position the jet plate. The thickness of the bakelite-made impingement plate was 15 mm. The bottom of the impingement plate was insulated with a fiberglass material. This fiberglass insulation material was supported by another bakelite-made plate with thickness of 20 mm. During jet impingement cooling, a 20 mm-thickness styrofoam was placed on the acrylic jet plate to reduce the heat loss. The heat loss from the jet plate might result in a decrease of the temperature of recirculation flow and consequently affects the heat transfer. This flow recirculation phenomenon will be explained later in this paper. During each measurement, it requires a two-hour waiting period for the system to reach a thermally steady-state condition. The measured temperatures were recorded by a HP-3856 data acquisition system. The experiment was conducted in a room with air conditioning. The room temperature was controlled within a deviation of ± 1.0 °C from the jet total temperature.

Eighty-eight experiments were arranged by varying the jet plate, air volumetric flow rate and heated-surface width. The heated-surface width was the same as the jet plate width. In this work, totally six jet plates were used. In four of them, the jet plate length (L) was 500 mm, but their jet diameters were individually 1.5, 3, 6 and 9 mm. For the other two, the jet diameter was 6 mm, but their jet plate lengths were individually 90 and 150 mm. For every individual experiment, by metering an appropriate air volumetric flow rate passing through the jet orifice, a desired jet Reynolds number was achieved. By wiring a different number (3, 5 or 7) of the heating foils in series and positioning the two removable bars (Fig. 1) individually at proper locations, a different heated-surface width was obtained. Fig. 3 shows the wiring of the heating foils. For instances, by connecting points 5A and 5B individually to the positive and negative connectors on the DC power supply, the inner five heating foils will be electrically arranged in series. This arrangement provides a heated-surface width of 62.5 mm.

4. Uncertainty analysis and comparison of experimental data

An uncertainty analysis was performed. In this experiment, there are two uncertainties relevant to the measured data. One resulted from the flow-rate measurement and the other arose from the heat transfer measurement. In the flow-rate measurement, a rotameter was used. According

to the manufacturer's supplied data, the inaccuracy of this rotameter would give rise to a maximum 5% error on the jet Reynolds number. In the heat transfer measurement, according to Eq. (1), both the inaccuracy due to the temperature measurement and the inaccuracy of the surface heat flux would result in the uncertainty of the local Nusselt number. In this work, the same thermocouple was used to measure the adiabatic and heated-wall temperatures. Moreover, the temperature difference between the middle heating foil and thermocouple was verified to be less than 0.05 °C. Thus in the analysis the inaccuracy of the temperature measurement was neglected. The inaccuracy of the surface heat flux was mainly attributed to radiation loss from heating foils (3.1%), non-uniformity of heating foils (4.4%), lateral solid heat conduction (2.0%) and heat loss through the insulation (0.9%). Based on the above data, the uncertainty of the measured Nusselt number was evaluated to be 5.81%.

Many experiments regarding to single jet impingement were performed in the past few decades. However, none of these experiments are the same as this work, which considers the jet after impingement restricted to flow only in two opposite directions. For purpose of comparison, a heat transfer measurement for an unconfined jet impinging on a flat plate was performed using the present experimental apparatus. These measured data were compared with those obtained by Goldstein and Franchett [9]. In their work, a liquid-crystal thermal-image technique was used and the thermal condition on their impingement plate was verified to fall between the conditions of constant heat flux and constant temperature. The comparison of the results is presented in Fig. 4. In the diagram, the solid line represents their correlation result. It reveals that, except for the region near to the stagnation point, the current obtained data are only slightly lower than theirs. The current measured data also indicates that the local Nusselt number would decrease with an increase of the heated-surface width. In our measurement, the width of the heated surface is smaller than theirs. If this width is enlarged, a better match between our data and their result in the region away from the stagnation point is expected. As indicated in Fig. 4, in the region near to the stagnation point, apparently their data are larger than ours. The largest discrepancy appears at the stagnation point. However, as their measured data [9] were carefully examined, it was found that their measured stagnation Nusselt number is 20% lower than their correlation result. The heat transfer characteristic in the region near to the stagnation point is different from that in the region far away from the stagnation point. Goldstein and Franchett [9] used a simple exponential function to fit entire spanwise local Nusselt number. Inevitably, a relatively large discrepancy between their measurement data and their correlation result would appear at the stagnation point. If their correlation is corrected, the deviation in Fig. 4 should be reduced.

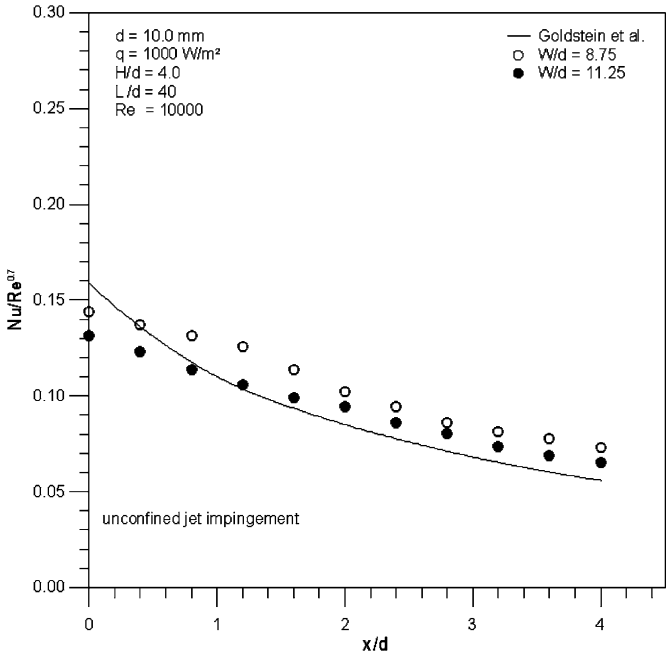

Fig. 4. Comparison of experimental data.

5. Results

The specifications of the 88 experiments were summarized in Table 1. For some of these experiments, the local Nusselt number distributions on the x-axis were measured. Fig. 5 shows two typical results of these measurements. Since the jet flow is symmetric about the y-axis, for simplicity, only the data on the positive x-axis are presented. In the diagram, $x/d = 0$ represents the location of the stagnation point. As shown, the local Nusselt number increases with the jet Reynolds number (Re). In the literature [14,17,19], for a jet impinging on a heated flat surface, two local maxima of Nusselt number were observed. The current result also shows that, for $Re = 30{,}000$, there appears two peaks on the local Nusselt number distribution. The first peak locates at $x/d \approx 1.0$ and the second peak can be roughly observed at $x/d \approx 2.4$. The first peak indicates the location of the transition point from impingement region to wall jet region; the second peak could be corresponding to the location having a strong turbulence

Table 1
Category of Experiments

Exp. No.	Re	H/d	W/d	L/d
1–3	15,000	1, 2, 4	6.25	5.5
4	15,000	2	10.42	16.7
5–8	10,000, 15,000	1	4.17, 6.94	27.8
9–20	10,000, 15,000	2, 4	4.17, 6.94, 9.72	27.8
21–23	15,000	1, 2, 4	10.42	33.3
24	30,000	1	10.42	33.3
25–26	15,000, 30,000	1	10.42	41.7
27–53	10,000, 15,000, 30,000	2, 4, 6	6.25, 10.42, 14.58	41.7
54–80	10,000, 15,000, 30,000	2, 4, 6	12.5, 20.83, 29.17	83.3
81–86	10,000, 15,000	2, 4, 6	25	166.7
87–88	10,000, 15,000	2	41.7	166.7

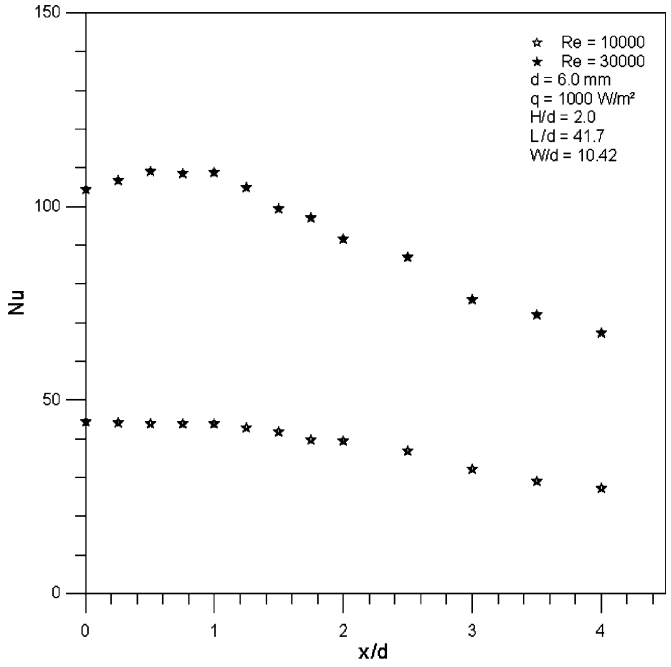

Fig. 5. Local Nusselt number distributions.

[17]. However, for $Re = 10{,}000$, the above phenomenon is not pronounced.

5.1. Effect of W/d on Nu_{sg}

Fig. 6(a) and (b) indicate that the stagnation Nusselt number (Nu_{sg}) decreases with an increase of the jet plate width-to-jet diameter ratio (W/d). But the decreasing rate decreases with an increase of the W/d.

Garimella and Rice [14] and Fitzgerald and Garimella [15] had shown that, for a confined jet impingement, a recirculation flow would form at up to 10 times the jet diameter downstream the jet centerline. This flow recirculation would bring the air in the downstream to the vicinity of the jet orifice. Due to entrainment effect, this recirculation flow would mix with the flow emanating from the jet orifice and affects the heat transfer. Moreover, the stronger the flow mixing or the higher the temperature of the air in the downstream, the greater the degradation of the heat transfer. In the considered jet plate-to-impingement plate configuration, the jet after impingement was restricted to flow only in two opposite directions parallel to the x-axis. An increase of the jet plate width means an increase of the heated-surface area in the direction (y-direction) perpendicular to the main flow. For a certain amount of air emanating from the jet orifice, this would give rise to a decrease of the air velocity in the downstream. In this work, a constant surface heat-flux condition was considered. This implies that the air temperature in the downstream would rise. As explained in the above, due to the flow-recirculation effect, this would cause the degradation of the heat transfer at the stagnation point. Thus, Fig. 6(a) and (b) indicate that the Nu_{sg} decreases with an increase of the W/d.

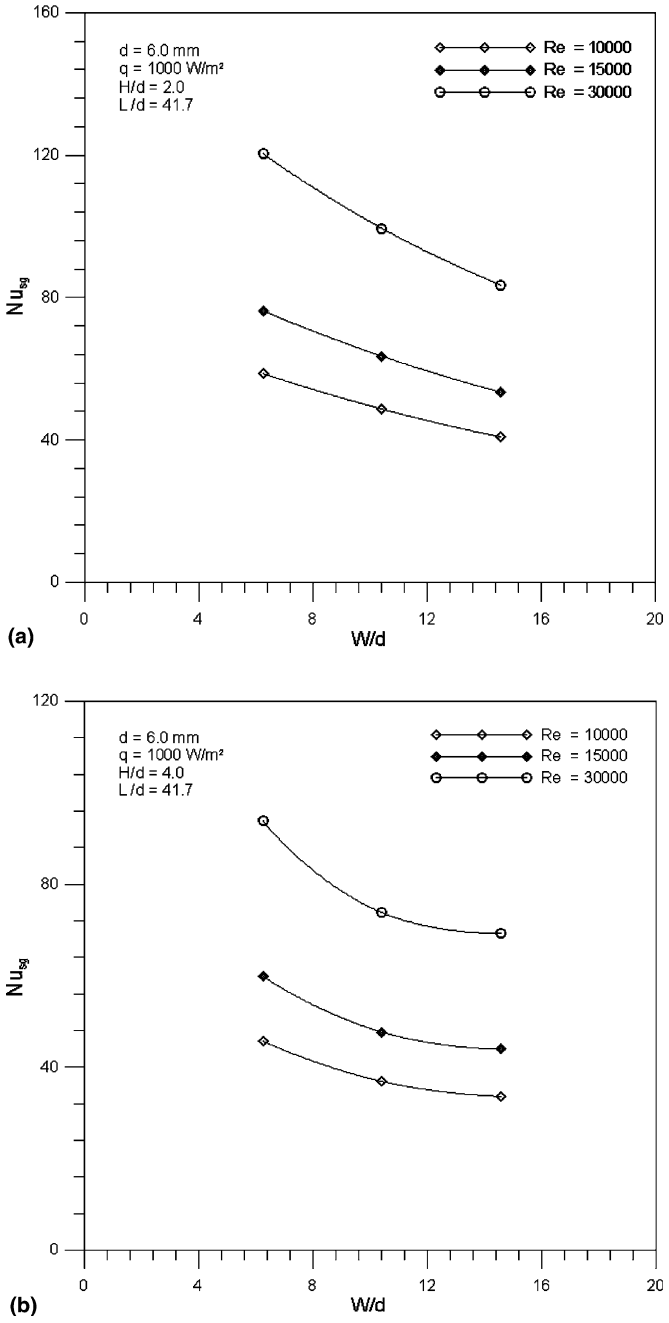

Fig. 6. Effect of W/d on Nu_{sg}: (a) $H/d = 2.0$, (b) $H/d = 4.0$.

5.2. Effect of L/d on Nu_{sg}

Fig. 7 indicates that the stagnation Nusselt number also decreases with an increase of the jet plate length-to-jet diameter ratio (L/d). Similar to the result shown in Fig. 6(a) and (b), the decreasing rate of the stagnation Nusselt number appears to decrease with an increase of the L/d. For an increase of the jet plate length, without varying the amount of air emanating from the jet orifice, basically the air temperature at the same location in the downstream would remain unchanged. However, as the jet plate length increases, the pressure difference between the jet

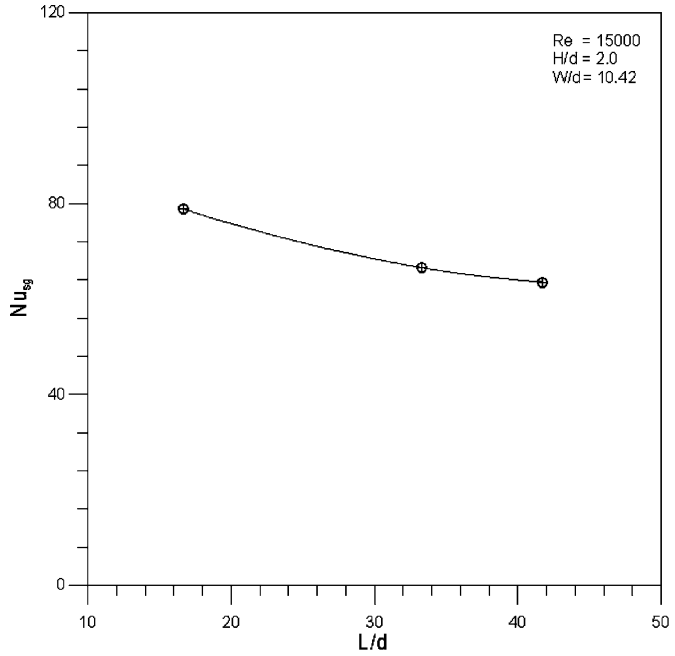

Fig. 7. Effect of L/d on Nu_{sg}.

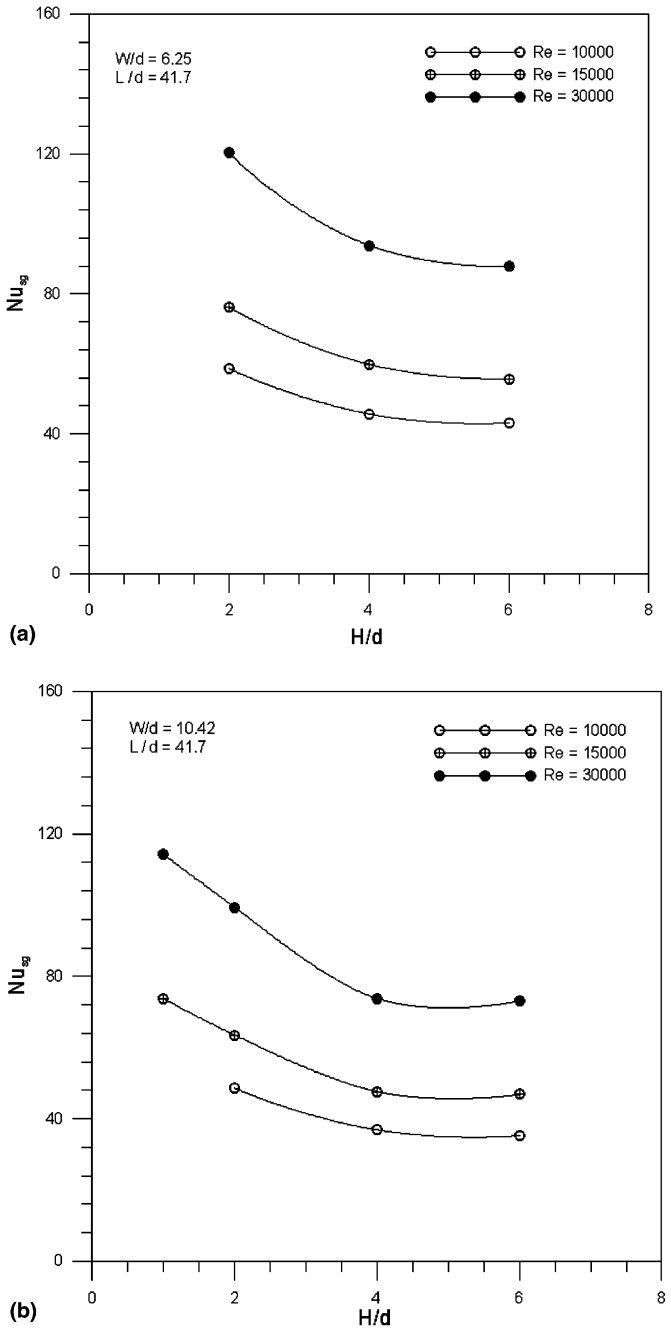

Fig. 8. Effect of H/d on Nu_{sg}: (a) $W/d = 6.25$, (b) $W/d = 10.42$.

and ambient air (outside the channel) would increase. This increase in the pressure difference is suspected to cause an enhancement of the flow mixing near the stagnation point. It eventually makes the stagnation Nusselt number decrease with an increase of the L/d.

Comparing Fig. 7 with Fig. 6(a) and (b), it shows that the effect of L/d on the stagnation Nusselt number is slightly weaker than that of W/d. As mentioned in the earlier, for an increase of the W/d, hotter air in the downstream would be brought to the vicinity of the jet orifice and mixes with the jet. This flow-recirculation and mixing process would degrade the heat transfer at the stagnation point. It has also been explained in the above, for an increase of the L/d, the decrease of the stagnation Nusselt number is simply considered to be due to an enhancement of the flow mixing near the stagnation point. However, for jet impingement, the flow mixing near the jet orifice originally is strong, thus the effect of this flow-mixing enhancement on the heat transfer is limited. This might render that the effect of L/d on the stagnation Nusselt number is weaker than that of W/d.

5.3. Effect of H/d on Nu_{sg}

Fig. 8(a) and (b) indicate that the stagnation Nusselt number decreases with an increase of the plate spacing-to-jet diameter ratio (H/d). A larger spacing between the jet plate and impingement plate allows a longer distance for the jet to mix with the recirculation flow before the jet reaches the impingement plate. This flow mixing would deteriorate the heat transfer. Thus the result shows that the stagnation Nusselt number decreases with an increase of the H/d.

Garimella and Rice [14] and Fitzgerald and Garimella [15] had investigated the effect of H/d on the stagnation Nusselt number. They found that, for the H/d less than 6.0, this effect is insignificant. Their result is different from that obtained in the present work. In their experiments, a small and discrete heated surface with dimensions of 10 mm by 10 mm, under a large jet plate, was considered. To such an experimental arrangement, the area covered by the jet plate would be much larger than the area of the heated surface. Thus the temperature of the recirculation air in their experiment should be lower than that in this work, provided that the same surface heat flux and

jet temperature were considered. Besides that, in their experiment the jet after impingement was free to flow in any radial direction; but in our experiment the jet was restricted to flow only in two opposite directions. Hence, in their jet impingement, the effect of flow mixing (between the jet and recirculation flow) on the stagnation Nusselt number would be smaller than that in our jet impingement. This could be the reason resulting in the deviation.

Gardon and Akfirat [22] had also investigated the effect of jet height on the stagnation Nusselt number for an unconfined two-dimensional jet impingement. An optimum jet height, approximately five times the hydraulic jet diameter, was found. This optimum jet height affords a maximum stagnation Nusselt number. The appearance of this maximum stagnation Nusselt number was attributed to an increase of the jet-centerline turbulence intensity with the jet height in the potential-core region. This renders that, for the jet height less than five times the hydraulic jet diameter (approximately the potential-core length), the stagnation Nusselt number increases with the jet height. This trend is different from those obtained by Garimella and Rice [14] and Fitzgerald and Garimella [15], and it is also converse to our result. In their experiment, an unconfined jet impinging on an isothermal plate was considered, thus the temperature of the reentry air through the entrainment effect could be much lower than that in our work. This might cause that, in their jet impingement, the effect of jet-centerline turbulence intensity on the stagnation Nusselt number becomes much stronger than that of flow mixing. Consequently, their result reveals a different dependence of the stagnation Nusselt number on jet height.

Sparrow et al. [5] had also investigated the effect of jet height on the impingement heat transfer for a jet in a cross flow. They also found a maximum Nusselt number for the H/d in the range 5–6. In their experiment, the total temperature of the cross flow is close to that of the jet. This cross flow would diminish the flow-recirculation effect. Thus the jet-centerline turbulence-intensity effect might dominate the dependence of the stagnation Nusselt number on H/d. Similar to the work performed by Gardon and Akfirat [22], it results in the appearance of the maximum Nusselt number.

The above results reveal that the dependence of the stagnation Nusselt number on H/d is quite complex. However, based on the comparisons, it may infer that the surface heating condition (boundary condition) on an impingement plate and the flow arrangement of a jet after impingement are two important factors governing the dependence of the stagnation Nusselt number on H/d.

Fig. 8(a) and (b) show that, for the H/d in the range 4.0–6.0, the influence of H/d on the stagnation Nusselt number is quite small. The potential-core length of a jet generally is 4–6 times the jet diameters. As the plate spacing approaches this length, near the stagnation point, the jet-centerline turbulence intensity would largely increase. As mentioned in the above, this would enhance the heat transfer at the stagnation point. Under this circumstance, the flow-mixing effect could be considerably offset by this jet-centerline turbulence-intensity effect. Thus the result shows that, for the H/d in the range 4.0–6.0, the effect of H/d on the stagnation Nusselt number is small.

6. Correlation of stagnation Nusselt number

As mentioned earlier, the stagnation Nusselt number for the confined jet impingement is a function of Re, H/d, W/d and L/d. Following is a brief description of the procedure in correlating the measured data.

Existing correlations express the Nusselt number for jet impingement as a function of Re^c [7,10–13]. The exponent, c, is a constant and it is in the range 0.45–0.8. In this work, the exponent for the jet Reynolds number was found to be 0.638. This value is consistent to that obtained in an earlier work [11] performed in the same laboratory.

In Fig. 9, the abscissa is $\ln(H/d)$ and the ordinate is $\ln(Nu_{sg}/Re^{0.638})$. After plotting the measured data into the diagram, those data with the same W/d and L/d values were successfully fitted into a straight line. For different sets of W/d and L/d values, different straight lines were obtained. As indicated, the slopes of all these straight lines are quite close to -0.3. This ensures that the relationship, $Nu_{sg} \propto (H/d)^{-0.3}$, exists.

In Fig. 10, the abscissa is W/d and the ordinate is $\ln\{Nu_{sg}/[Re^{0.638}(H/d)^{-0.3}]\}$. As the measured data were plotted into the diagram, those data with the same L/d value were also successfully fitted into a straight line. Similarly, for different L/d values, different straight lines were obtained. Moreover, the slopes of all these straight lines were also quite close. In the analysis, a common slope, equal to -0.044, was selected. This means that the stagna-

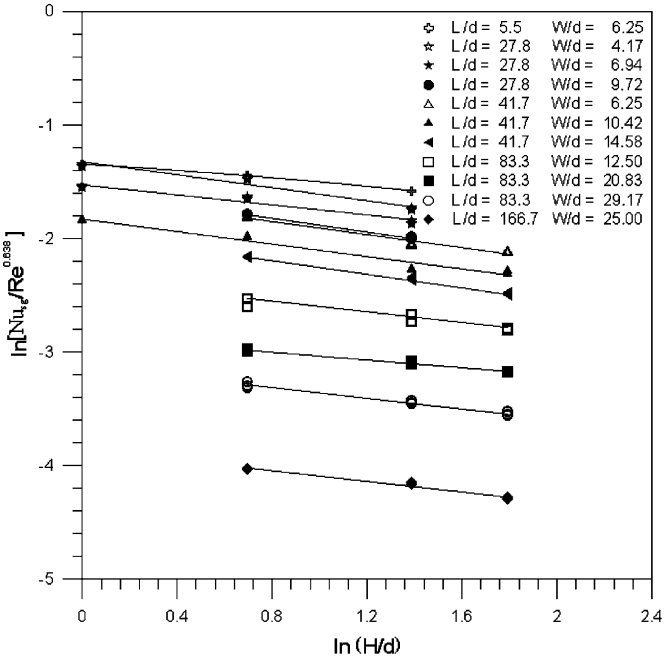

Fig. 9. $\ln(Nu_{sg}/Re^{0.638})$ versus $\ln(H/d)$.

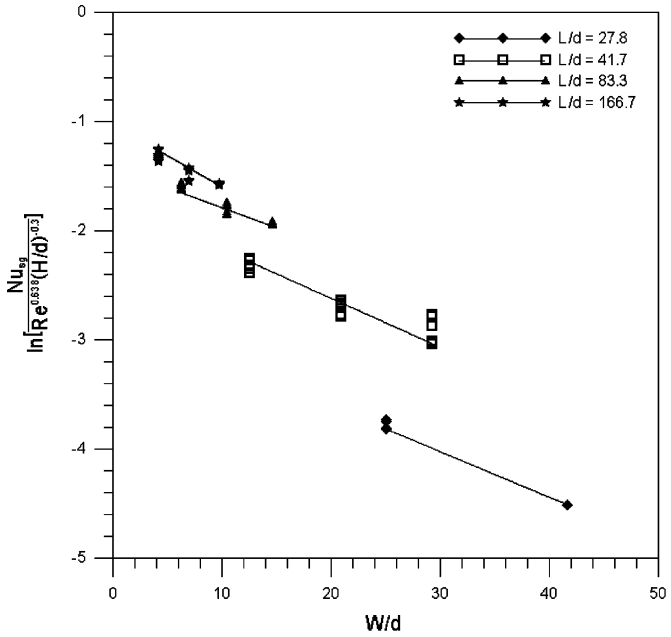

Fig. 10. $\ln\{Nu_{sg}/[Re^{0.638}(H/d)^{-0.3}]\}$ versus W/d.

tion Nusselt number was set proportional to an exponential function with exponent of $[-0.044(W/d)]$. However, it has to mention here that in this work the available experimental data in the low L/d range were not sufficient. Thus Fig. 10 was plotted only based on the data with the L/d value in the range 27.8–166.7.

After accomplishing the correlations of the stagnation Nusselt number with Re, H/d and W/d, all the 88 sets of measured data were plotted into a diagram with L/d as the abscissa and $\ln\{Nu_{sg}/[Re^{0.638}(H/d)^{-0.3}e^{-0.044(W/d)}]\}$ as the ordinate. The result is shown in Fig. 11. As indicated,

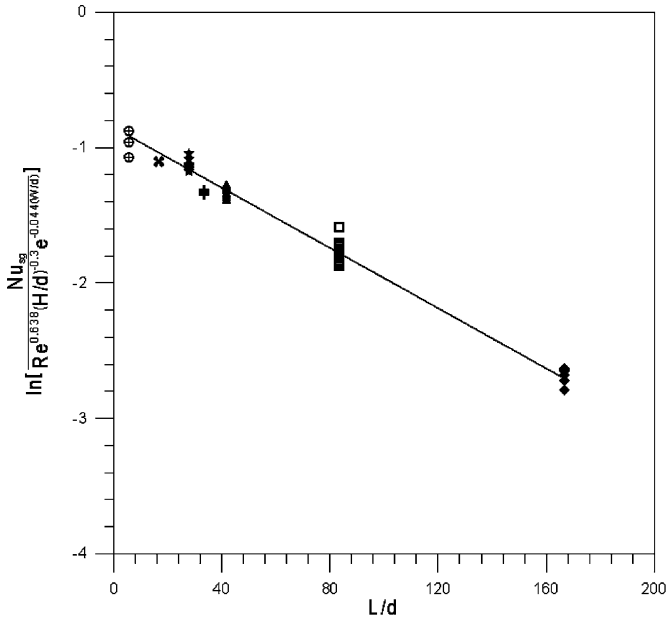

Fig. 11. $\ln\{Nu_{sg}/[Re^{0.638}(H/d)^{-0.3}e^{-0.044(W/d)}]\}$ versus L/d.

all the measured data were also fitted well into a straight line. The slope of this straight line is -0.011, and its intersection with the ordinate corresponds to a value of 0.426.

Based on the above analysis, a complete correlation for the stagnation Nusselt number was found and it can be expressed as follows:

$$Nu_{sg} = 0.426Re^{0.638}(H/d)^{-0.3}e^{-[0.044(W/d)+0.011(L/d)]} \quad \text{for} \quad \begin{matrix} 10{,}000 \leqslant Re \leqslant 30{,}000, & 1 \leqslant H/d \leqslant 6 \\ 4.17 \leqslant W/d \leqslant 41.7, & 5.5 \leqslant L/d \leqslant 166.7 \end{matrix} \tag{2}$$

Eq. (2) can be used to predict the stagnation Nusselt number in the indicated range of operating conditions. In the analysis, the deviations between the measured data and corresponding predicted values were evaluated. The result shows that the mean deviation is 6% and maximum deviation is 16.9%. This maximum deviation occurs at $Re = 15{,}000$, $H/d = 1$, $W/d = 6.25$ and $L/d = 5.5$. At this operating condition, the predicted value is greater than the measured data.

7. Conclusions

For the jet Reynolds number (Re) of 30,000, the transition of the confined jet from impingement region to wall-jet region can be observed from a peak Nusselt number in the flow direction. This transition locates at $x/d \approx 1.0$. A secondary peak Nusselt number can also be roughly observed at $x/d \approx 2.4$. For $Re = 10{,}000$, these two peaks cannot be clearly observed from the Nusselt number distribution.

The stagnation Nusselt number increases with the Re, but decreases with an increase of the jet plate width-to-jet diameter ratio (W/d) and jet plate length-to-jet diameter ratio (L/d). The considered jet plate-to-impingement plate configuration restricts the jet after impingement to flow only in two opposite directions (aligned to the direction of jet plate length). It turns out that the influence of W/d on the stagnation Nusselt number is stronger than that of L/d.

It is known that, in the potential-core region, the jet-centerline turbulence intensity increases with the plate spacing-to-jet diameter ratio (H/d). This would result that the stagnation Nusselt number increases with the H/d. For the confined jet impingement, the flow mixing between the jet and recirculation flow is believed to be another factor affecting the dependence of the stagnation Nusselt number on H/d. As the H/d increases, the flow-mixing length also increases. This would result in a decrease of the stagnation Nusselt number. Moreover, the higher the recirculation flow temperature, the stronger the effect of flow mixing on the stagnation Nusselt number. In this work, a restricted-flow arrangement and a continuous heated surface were considered. This might cause that, for an increase of the H/d, the flow-mixing effect is stronger than the jet-centerline turbulence intensity effect. Thus the result reveals that the stagnation Nusselt number decreases with an increase of the H/d.

The stagnation Nusselt number was successfully correlated into a simple equation using the limited experimental data. It is a function of the 0.638 power of the Re. The H/d, W/d and L/d were verified to be the other three parameters affecting the stagnation Nusselt number. The result shows that the stagnation Nusselt number is proportional to the -0.3 power of the H/d. It is also proportional to an exponential function with exponent of $[-0.044(W/d) - 0.011(L/d)]$.

References

[1] K. Jambunathan, E. Lai, M.A. Moss, B.L. Button, A review of heat transfer data for single circular jet impingement, Int. J. Heat Fluid Flow 13 (2) (1992) 106–115.

[2] R.J. Goldstein, A.I. Behbahani, Impingement of a circular jet with and without crossflow, Int. J. Heat Mass Transfer 25 (9) (1982) 1377–1382.

[3] R.J. Goldstein, A.I. Behbahani, K.K. Heppelmann, Streamwise distribution of the recovery factor and the local heat transfer coefficient to an impinging circular air jet, Int. J. Heat Mass Transfer 29 (1986) 1227–1235.

[4] J.P. Bouchez, R.J. Goldstein, Impingement cooling from a circular jet in a cross flow, Int. J. Heat Mass Transfer 13 (1975) 719–730.

[5] E.M. Sparrow, R.J. Goldstein, M.A. Rouf, Effect of nozzle surface separation distance on impingement heat transfer for a jet in a crossflow, J. Heat Transfer 97 (1975) 528–533.

[6] R.J. Goldstein, K.A. Sobolik, W.S. Seol, Effect of entrainment on the heat transfer to a heated circular air jet impinging on a flat surface, J. Heat Transfer 112 (1990) 608–611.

[7] E.M. Sparrow, Z.X. Xu, L.F.A. Azevedo, Heat (mass) transfer for circular jet impingement on a confined disk with annular collection of the spent air, J. Heat Transfer 109 (1987) 329–335.

[8] R.J. Goldstein, J.F. Timmers, Visualization of heat transfer from arrays of impinging jets, Int. J. Heat Mass Transfer 25 (12) (1982) 1857–1868.

[9] R.J. Goldstein, M.E. Franchett, Heat transfer from a flat surface to an oblique impinging jet, J. Heat Transfer 110 (1988) 84–90.

[10] L. Huang, M.S. EL-Genk, Heat transfer of an impinging jet on a flat surface, Int. J. Heat Mass Transfer 37 (13) (1994) 1915–1923.

[11] J.Y. San, C.H. Huang, M.H. Shu, Impingement cooling of a confined circular air jet, Int. J. Heat Mass Transfer 40 (6) (1997) 1355–1364.

[12] D. Lytle, B.W. Webb, Air jet impingement heat transfer at low nozzle-plate spacing, Int. J. Heat Mass Transfer 37 (12) (1994) 1687–1697.

[13] C.Y. Li, S.V. Garimella, Prandtl-number effects and generalized correlations for confined and submerged jet impingement, Int. J. Heat Mass Transfer 44 (2001) 3471–3480.

[14] S.V. Garimella, R.A. Rice, Confined and submerged liquid jet impingement heat transfer, J. Heat Transfer 117 (1995) 871–877.

[15] J.A. Fitzgerald, S.V. Garimella, A study of the flow field of a confined and submerged impinging jet, Int. J. Heat Mass Transfer 41 (1998) 1025–1034.

[16] M. Angibletti, R.M. Di Tommaso, E. Nino, G. Ruocco, Simultaneous visualization of flow field and evaluation of local heat transfer by transitional impinging jet, Int. J. Heat Mass Transfer 46 (2003) 1703–1713.

[17] V. Narayanan, J. Seyed-Yagoobi, R.H. Page, An experimental study of fluid mechanics and heat transfer in an impinging slot jet flow, Int. J. Heat Mass Transfer 47 (2004) 1827–1845.

[18] D.W. Zhou, S.J. Lee, Heat transfer enhancement of impinging jets using mesh screens, Int. J. Heat Mass Transfer 47 (2004) 2097–2108.

[19] A.M. Huber, R. Viskanta, Effect of jet-jet spacing on convective heat transfer to confined impinging arrays of axisymmetric air jets, Int. J. Heat Mass Transfer 37 (18) (1994) 2859–2869.

[20] J.Y. San, M.D. Lai, Optimum jet-to-jet spacing of heat transfer for staggered arrays of impinging air jets, Int. J. Heat Mass Transfer 44 (2001) 3997–4007.

[21] B.P. E Dano, J.A. Liburdy, K. Kanokjaruvijit, Flow characteristics and heat transfer performance of a semi-confined impinging array of jet: effect of nozzle geometry, Int. J. Heat Mass Transfer 48 (2005) 691–701.

[22] R. Gardon, J.C. Akfirat, Heat transfer characteristics of impinging two-dimensional air jets, J. Heat Transfer 88 (1966) 101–108.